Workshop on Statistical modeling for shapes and imaging

Shape representation as distribution of geometric features: from currents to oriented varifolds

Irène Kaltenmark
Inria - Institut de Mathématiques de Bordeaux
Université de Bordeaux

joint work with Nicolas Charon and Benjamin Charlier

March 2019

Outline

Shape Spaces [Grenander, Miller, Trouvé, Younes, Beg, ..., Arguillère]

Define a metric on a space of shapes

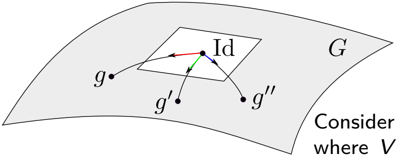

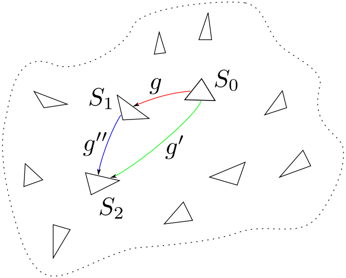

$$d(S_0, S_1) \doteq \inf\{d_G(\mathrm{Id}, g) \,|\, g \cdot S_0 = S_1\}\,.$$

Consider $G \doteq \{\psi_1^v \,|\, v \in L^2([0,1], V)\}$ where V is a space of vector fields on a fixed *ambient space*, e.g. $\mathbb{R}^n$, and

$$\psi_t^v = \mathrm{Id} + \int_0^t v_s \circ \psi_s^v \, ds\,.$$

G is equipped with a distance:

$$d_G(\mathrm{Id}, \psi) \doteq \inf\{\int_0^1 |v_t|_V^2 \, dt \,|\, \psi_1^v = \psi\}\,.$$

G acts on $\mathcal{S}(\mathbb{R}^n)$: $\psi \cdot S = \psi(S)$ and induces an infinitesimal action of V on $\mathcal{S}(\mathbb{R}^n)$:

$$\xi(S) : V \to T_S\mathcal{S}(\mathbb{R}^n), v \mapsto v \cdot S = v(S)\,.$$

Strength: this approach handles a large type of shape data and combines definition of distances with shape registration

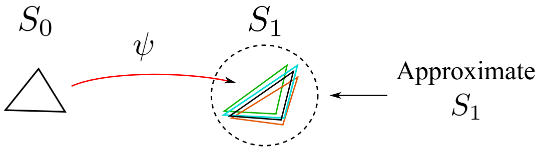

Inexact matching problem:

$$E(v) = \frac{1}{2}\int_0^1 |v_t|_V^2 \, dt + \frac{\lambda}{2} D(\psi(S_0), S_1)^2$$

Data attachment term: currents and varifolds model shapes as distributions of their local tangent or normal vectors [Glaunès 05, Charon 13]. Reproducing kernels of Hilbert spaces lead to various types of **data fidelity metrics between shapes that do not depend on the parametrization**.
Framework presented here: the choice of the metric reduces to one or two scalar functions.

Related work: normal cycles [Roussillon 16], optimal transport as data term [Feydy 17], square-root velocity (SRV) representation [Srivastava 09, 12]

Back to simple functions

How to evaluate f ?

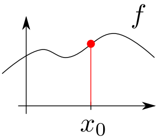

$f(x_0)$

Dirac at x_0

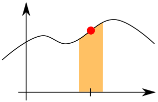

$\int_{B(x_0)} f(x)dx$

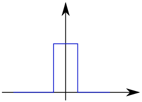

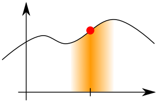

$\int_{\mathbb{R}} f(x)\varphi(||x - x_0||)dx$

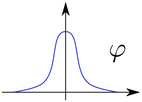

Properties of the test functions :

- Scale (e.g. for Gaussian distributions)
- Shape of the tail

Shapes as distributions

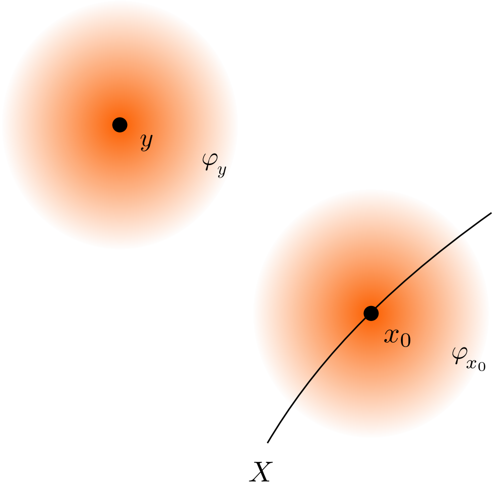

$$\int_X \varphi(||x - x_0||) d\mathrm{vol}^X(x) \approx \text{mass of } X \text{ around } x_0 \,,$$

$$\int_X \varphi(||x - y||) d\mathrm{vol}^X(x) = 0 \,.$$

Shapes duality

Functions	Shapes	RKHS approach
$I_f \in \mathcal{D}'$	$\mu_X \in \mathcal{D}'$	$\mu_X \in \mathcal{H}'$
$\uparrow$	$\uparrow$	$\updownarrow$
$\varphi \in \mathcal{D}$	$\omega \in \mathcal{D}$	$\varphi_X \in \mathcal{H}$
$f : \mathbb{R} \to \mathbb{R}$	X (submanifold)	X (submanifold)

$$I_f(\varphi) = \int_{\mathbb{R}} f\varphi \qquad \mu_X(\omega) = \int_X \omega(x) d\mathrm{vol}^X(x)$$

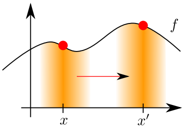

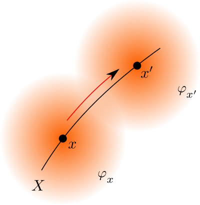

General kernel:

$$X \longleftrightarrow \varphi_X = \int_X \varphi_x$$

Degenerate kernel (Dirac) :

$$X \longleftrightarrow \mathbb{1}_X = \int_X \delta_x$$

Shapes duality

		RKHS approach
$I_f \in \mathcal{D}'$	$\mu_X \in \mathcal{D}'$	$\mu_X \in \mathcal{H}'$
$\uparrow$	$\uparrow$	$\updownarrow$
$\varphi \in \mathcal{D}$	$\omega \in \mathcal{D}$	$\varphi_X \in \mathcal{H}$
$f : \mathbb{R} \to \mathbb{R}$	X (submanifold)	X (submanifold)

$I_f(\varphi) = \int_{\mathbb{R}} f\varphi$ $\quad$ $\mu_X(\omega) = \int_X \omega(x) d\mathrm{vol}^X(x)$

For two shapes X, Y, we have

$$\langle \mu_X, \mu_Y \rangle_{\mathcal{H}'} = \langle \varphi_X, \varphi_Y \rangle_{\mathcal{H}} .$$

For two points $x_0, y_0 \in \mathbb{R}^n$

$$\langle \delta_{x_0}, \delta_{y_0} \rangle_{\mathcal{H}'} = \varphi(||y_0 - x_0||_{\mathbb{R}^n}) .$$

Note that here $\varphi : \mathbb{R} \to \mathbb{R}$ (equivariance to rigid motion), e.g. $\varphi(u) = \exp(-u^2/\sigma^2)$.

Scalar product and norm

$$\langle \mu_X, \mu_Y \rangle_{\mathcal{H}'} = \int_Y \int_X \varphi(||y - x||) d\mathrm{vol}^X(x) d\mathrm{vol}^Y(y) = \mu_Y(\varphi_X)\,.$$

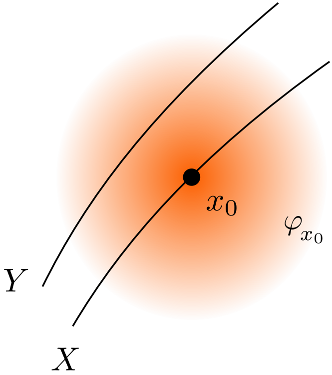

μ_Y acts linearly on φ_{x_0} :
it integrates the mass of Y in a neighborhood of x_0

$$\mu_Y(\varphi_{x_0}) = \int_Y \varphi(||y - x_0||) d\mathrm{vol}^Y(y)\,.$$

X and Y are similar around x_0 if

$$\mu_Y(\varphi_{x_0}) \approx \mu_X(\varphi_{x_0})\,.$$

.

Finally, $d(X, Y)^2 \doteq ||\mu_X - \mu_Y||^2_{\mathcal{H}'} = ||\mu_X||^2 - 2\langle \mu_X, \mu_Y \rangle + ||\mu_Y||^2\,.$

Discretization

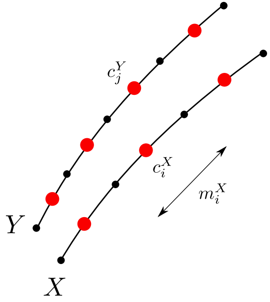

$$\langle \mu_{X_i}, \mu_{Y_j} \rangle = \int_{Y_j} \int_{X_i} \varphi(||y - x||) d\mathrm{vol}^X(x) d\mathrm{vol}^Y(y)$$

$$\approx m_i^X \int_{Y_j} \varphi(||y - c_i^X||) d\mathrm{vol}^Y(y)$$

$$\approx m_i^X m_j^Y \varphi(||c_j^Y - c_i^X||)$$

$$\langle \mu_X, \mu_Y \rangle \approx \sum_{i,j} m_i^X m_j^Y \varphi(||c_j^Y - c_i^X||)$$

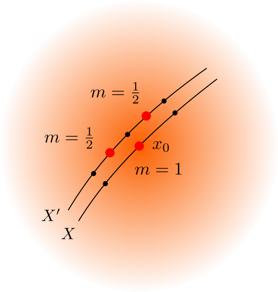

$$\langle \mu_{X_0}, \mu_X \rangle \approx 1 \times \varphi(0)$$

$$\langle \mu_{X_0}, \mu_{X'} \rangle \approx \left(\frac{1}{2} + \frac{1}{2} \right) \times \varphi(0)$$

If the diameters of the faces are small wrt to the scale of φ (how flat is φ around 0), the associated metric is **robust to parametrization**.

Discretization

- This metric induces registration algorithms that do not require pointwise correspondences between shapes.
  For example, one can register a curve with 100 points on a curve with 150 points.

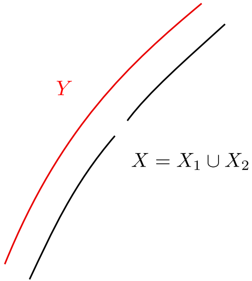

- Shapes union: if $X = X_1 \cup X_2$, then

$$\mu_X = \mu_{X_1} + \mu_{X_2} - \mu_{X_1 \cap X_2} \,.$$

- This metric is quite robust to discontinuities.
  Conversely, normal cycles allow to discriminate topological properties [Roussillon 16].

Mass sensitivity

$$\mu_Y \approx 2\mu_X$$

so that $d(X,Y)^2 = ||\mu_X - \mu_Y||^2 \approx ||\mu_X||^2$

Application to brain registration

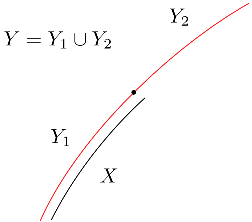

Inclusion detection ?

"$d(X,Y)^2 \approx ||\mu_{Y_2}||^2$"

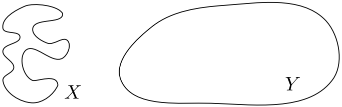

X and Y have the same length but

"$||\mu_X|| > ||\mu_Y||$"

This is not without consequences

Data compression

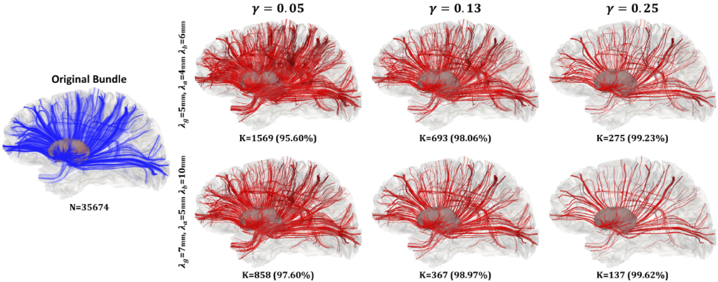

[Gori 17]

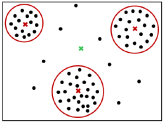

Cross section of 3 fiber bundles

Consider a fiber bundle $B = \bigcup_i^n X_i$ such that for any i, X_i is close to an average fiber $\tilde{X}$, i.e.

$$\mu_{X_i} \approx \mu_{\tilde{X}} ,$$

then

$$\mu_B = \sum_i^n \mu_{X_i} \approx n\mu_{\tilde{X}} .$$

Outline

Limitations

The tangent space distributions of shapes highlight natural correspondences...

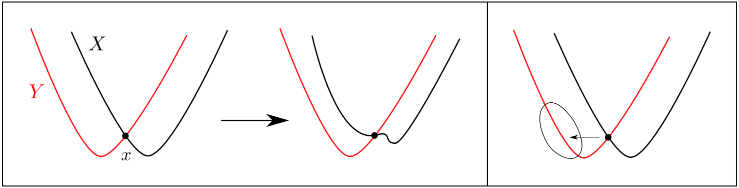

as well as the shapes' orientation:

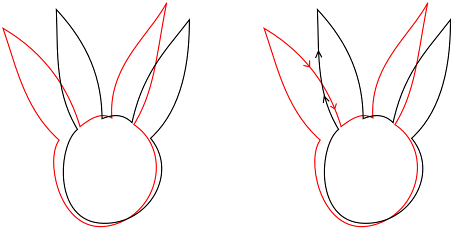

Tangent bundle

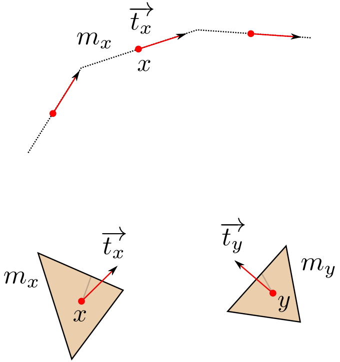

For curves and surfaces in $\mathbb{R}^2$ or $\mathbb{R}^3$, oriented tangent spaces can be represented by a unique unit vector (tangent or normal).

μ_X is now a distribution on a space of test functions $\omega : \mathbb{R}^n \times \mathbb{S}^{n-1} \to \mathbb{R}$, $(n = 2, 3)$:

$$\mu_X(\omega) = \int_X \omega(x, \overrightarrow{t_x}) d\mathrm{vol}^X(x)$$

$$\langle \delta_x^{\overrightarrow{t_x}}, \delta_y^{\overrightarrow{t_y}} \rangle_{\mathcal{H}'} = \varphi(||y - x||_{\mathbb{R}^n}) \gamma(\langle \overrightarrow{t_x}, \overrightarrow{t_y} \rangle_{\mathbb{R}^n}) \, .$$

Note that $\varphi : \mathbb{R} \to \mathbb{R}$, $\gamma : \mathbb{R} \to \mathbb{R}$ (equivariance to rigid motion).

Representation choices

X, Y two shapes, μ_X, μ_Y the respective distributions of their local tangent or normal vectors

$$\begin{aligned}\langle \mu_X, \mu_Y \rangle_{\mathcal{H}'} &= \iint_{X \times Y} \varphi(||y-x||_{\mathbb{R}^n}) \gamma(\langle \overrightarrow{t_x}, \overrightarrow{t_y} \rangle_{\mathbb{R}^n}) d\mathrm{vol}^X(x) d\mathrm{vol}^Y(y) \\ &\approx \sum_{i,j} m_i^X m_j^Y \varphi(||c_j^Y - c_i^X||) \gamma(\langle \overrightarrow{t_i^X}, \overrightarrow{t_j^Y} \rangle)\end{aligned}$$

Data type	$\gamma(\langle \overrightarrow{t_x}, \overrightarrow{t_y} \rangle)$	$\gamma(u)$
Currents [Glaunès 05]	$\langle \overrightarrow{t_x}, \overrightarrow{t_y} \rangle$	u
(unoriented) Varifolds [Charon 13]	$\langle \overrightarrow{t_x}, \overrightarrow{t_y} \rangle^2$	u^2
Oriented Varifolds*	$\exp\left(2\langle \overrightarrow{t_x}, \overrightarrow{t_y} \rangle / \sigma_T^2\right)$	$\exp\left(2u/\sigma_T^2\right)$
	$\propto \exp\left(-\lvert \overrightarrow{t_x} - \overrightarrow{t_y} \rvert^2 / \sigma_T^2\right)$	

Remark: σ_T does not depend on the scale of the shapes.

*[Kaltenmark,Charlier,Charon 17]

Representation choices

X, Y two shapes, μ_X, μ_Y the respective distributions of their local tangent or normal vectors

$$\langle \mu_X, \mu_Y \rangle_{\mathcal{H}'} = \iint_{X \times Y} \varphi(||y - x||_{\mathbb{R}^n}) \gamma(\langle \overrightarrow{t_x}, \overrightarrow{t_y} \rangle_{\mathbb{R}^n}) d\mathrm{vol}^X(x) d\mathrm{vol}^Y(y)$$

$$\approx \sum_{i,j} m_i^X m_j^Y \varphi(||c_j^Y - c_i^X||) \gamma(\langle \overrightarrow{t_i^X}, \overrightarrow{t_j^Y} \rangle)$$

Data type	$\gamma(\langle \overrightarrow{t_x}, -\overrightarrow{t_x} \rangle)$	
Currents [Glaunès 05]	$-\gamma(\langle \overrightarrow{t_x}, \overrightarrow{t_x} \rangle)$	$= -1$
(unoriented) Varifolds [Charon 13]	$\gamma(\langle \overrightarrow{t_x}, \overrightarrow{t_x} \rangle)$	$= 1$
Oriented Varifolds*	$\gamma(\langle \overrightarrow{t_x}, -\overrightarrow{t_x} \rangle)$	$= 0$

*[Kaltenmark,Charlier,Charon 17]

Current regularization

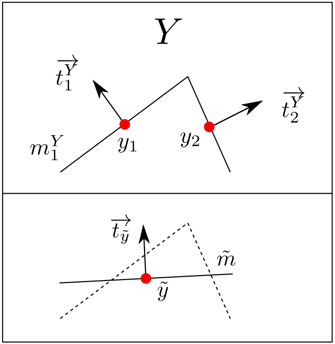

$$\langle \delta_x^{\overrightarrow{t_x}}, \mu_Y \rangle_{\mathcal{H}'} = \sum_{i=1}^{2} m_i^Y \varphi(||y_i - x||) \langle \overrightarrow{t_x}, \overrightarrow{t_i^Y} \rangle$$
$$\approx \varphi(0) \langle \overrightarrow{t_x}, m_1^Y \overrightarrow{t_1^Y} + m_2^Y \overrightarrow{t_2^Y} \rangle$$
$$\approx \tilde{m} \varphi(||\tilde{y} - x||) \langle \overrightarrow{t_x}, \overrightarrow{t_{\tilde{y}}} \rangle$$
$$\approx \langle \delta_x^{\overrightarrow{t_x}}, \tilde{m} \delta_{\tilde{y}}^{\overrightarrow{t_{\tilde{y}}}} \rangle_{\mathcal{H}'}$$

Mass cancellation effect: if $m_1^Y \overrightarrow{t_1^Y} + m_2^Y \overrightarrow{t_2^Y} \approx 0$, then $||\mu_Y||_{\mathcal{H}'} \approx 0$.

Counterpart: thin and sharp structures are not seen by the metric or at best their mass is underestimated, e.g. tails, tip of horns, leaf stem, etc.

Mass conservation with varifolds

Theorem (Charon 13)

*If φ and γ are two continuous **positive** functions, $\varphi(0) > 0$, and $\gamma(1) > 0$, then there exists $c > 0$, such that for any k-dimensional compact submanifold X*

$$c\,vol^k(X) \leq ||\mu_X||_{\mathcal{H}'}\,.$$

Applications in the diffeomorphometric framework

Inexact matching problem: deform a shape S_0 towards a target shape S_1

$$E(v) = \frac{1}{2}\int_0^1 |v_t|_V^2\, dt + \frac{\lambda}{2}|\mu_{\psi_1(S_0)} - \mu_{S_1}|_{\mathcal{H}'}^2$$

This energy is minimized by a gradient descent. Each step consists in:

- Computing the gradient of the data attachment term
- Pulling it backward over time
- Updating $t \to v_t$
- Updating $\psi_1(S_0)$ (end point of the geodesic generated by v)

Denoising with currents

Source: blue. Target: red.

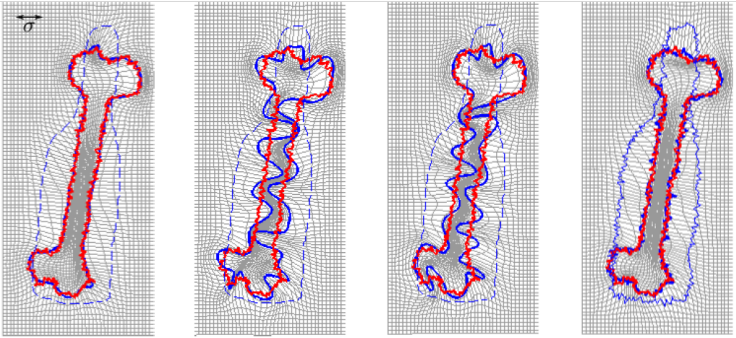

Current | Unoriented varifold | Oriented varifold | Noisy template

Denoising with currents

Source: green. Target: red.

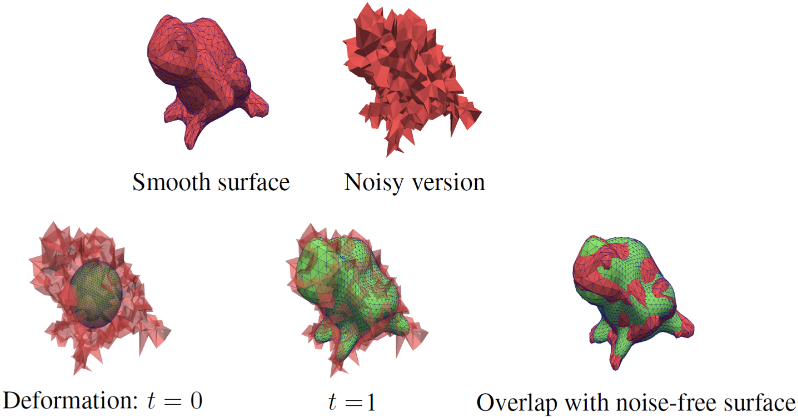

Comparisons

Source: blue. Target: red.

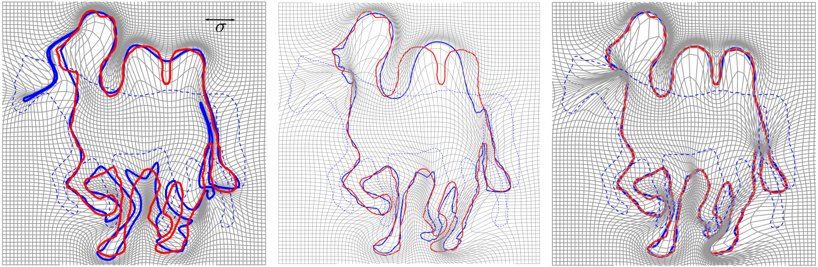

Currents Unoriented varifolds Oriented varifolds

Unoriented varifolds and multi-attachment terms

Source: blue. Target: red.

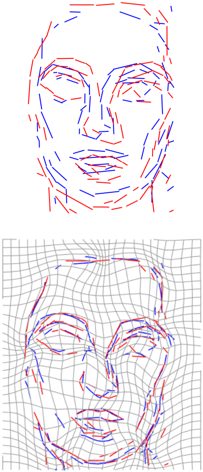

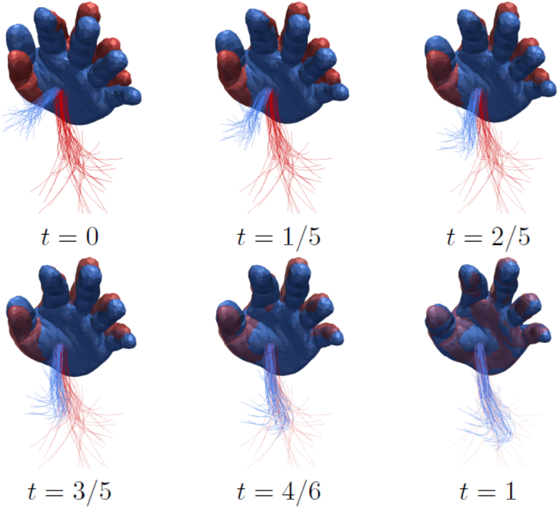

Restoration with oriented varifolds

Source: blue. Target: red.

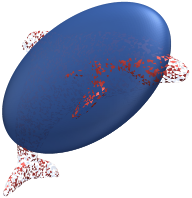

Initial shape is
an ellipsoid

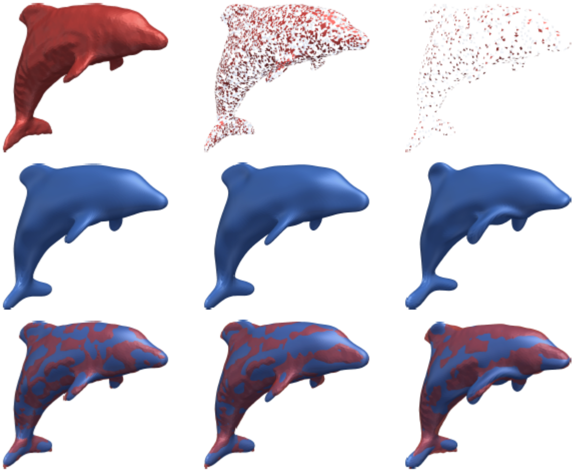

$p = 100\%$ $p = 30\%$ $p = 5\%$

Functional shapes

Consider two shapes $X, Y \subset \mathbb{R}^n$, respectively equipped with a signal $f^X : X \to \mathbb{R}^d$, $f^Y : Y \to \mathbb{R}^d$, then one can define

$$\langle \mu_{(X,f^X)}, \mu_{(Y,f^Y)} \rangle_{\mathcal{H}'} =$$
$$\iint_{X\times Y} \varphi(||y-x||_{\mathbb{R}^n})\gamma(\langle \overrightarrow{t_x}, \overrightarrow{t_y}\rangle_{\mathbb{S}^{n-1}}){\color{red}\varphi^f(||f^Y(y)-f^X(x)||_{\mathbb{R}^d})}d\mathrm{vol}^X(x)d\mathrm{vol}^Y(y)$$

[Charon 14]

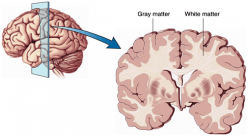

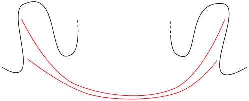
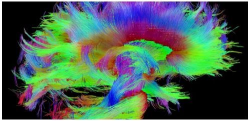

Clustering fibers under the constraint: take into account the ending points of the fibers [Gori 17]

Examples of signal: thickness/pressure measurements, brain activity map, etc.

Functional shapes

- Computing the previous metric for functional shape is straightforward
- Plug your new favorite metric in a deformation framework:
  - Do the deformations act on the feature ? (yes: $d\Phi(x) \cdot \overrightarrow{t_x}$, no: labels from segmentation)
  - Do you need an independant action on the feature/signal ? (metamorphosis).
  For registration allowing signal deformation, see *Fshapes Toolkit* [Charon, Charlier 15,18]

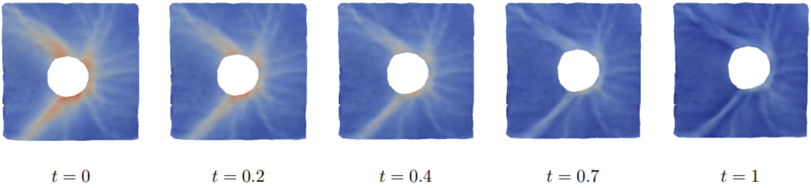

Matching of 2 membranes in the retina with thickness measurements.

Mass sensitivity

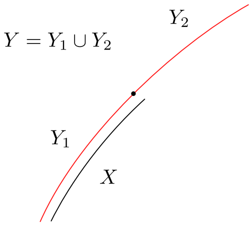

Inclusion detection ?

$$"d(X,Y)^2 \approx ||\mu_{Y_2}||^2"$$

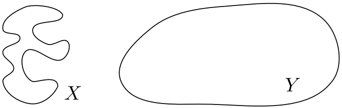

X and Y have the same length but

$$"||\mu_X|| > ||\mu_Y||"$$

This is not without consequences

Mass sensitivity

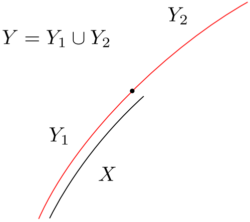

Inclusion detection ?

$$"d(X, Y)^2 \approx ||\mu_{Y_2}||^2"$$

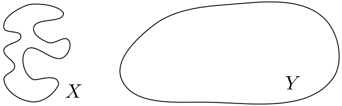

X and Y have the same length but

$$"||\mu_X|| > ||\mu_Y||"$$

This is not without consequences

Interlude

Jean Feydy

CMLA, ENS de Cachan

Conclusion - Why two metrics ?

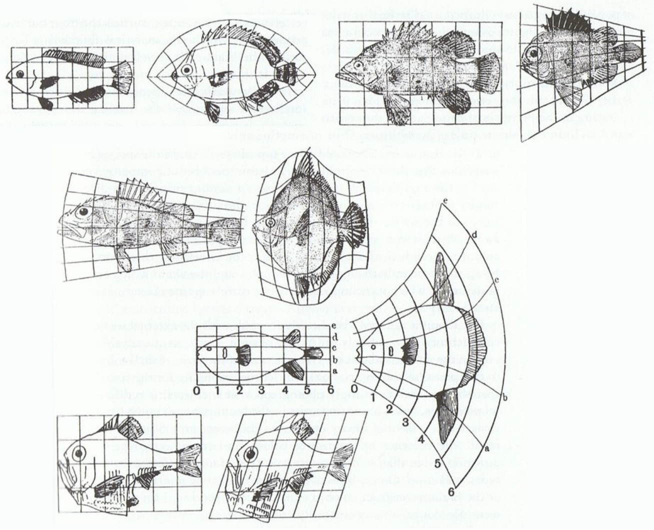

On Growth and Form, D'Arcy Thompson, 1917.

Conclusion - What global model for computational anatomy ?

Assumption: the geometry gives enough prior to retrieve the biological homologies between shapes

True → **False**

Low variability Local changes	Medium variability	High variability Complex phenomena
Kernel metrics+LDDMM	OT+LDDMM [Feydy et al.]	Priors on deformations [Gris] Elastic model for thickness estimation [Younes] Growth model with priors on the biological process [Kaltenmark] Etc.

Conclusion

Currents and varifolds metrics can be used in many applications *outside the diffeomorphometry framework* ! For example, to replace the Dice coefficient

$$c = \frac{2|X \cap Y|}{|X| + |Y|}\,.$$

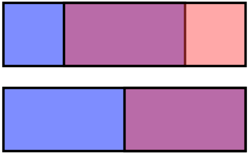

Top: red and blue have same area. Bottom: blue is twice larger than red.

Code: **Fshapes Toolkit** (Matlab) [Charlier, Charon]. You can customize very simply the functions φ and γ !
The next talk will introduce the KeOps library [Charlier, Feydy, Glaunès]!

Expedition in a non Diffeomorphic World

Growth and homology issues

Longitudinal data

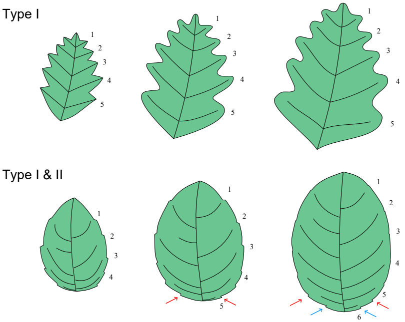

(a) Plant growth

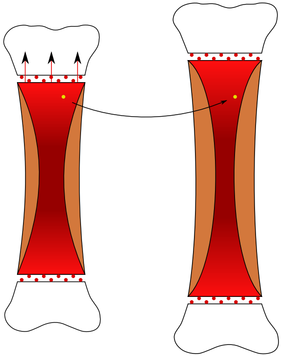

(b) Bone growth

On the macroscopic scale, one can identify two main types of growth process:

- Type I: a growth homogeneously distributed.
- Type II: a growth process that involves new material on specific areas (e.g. plant growth, crystal growth or mineralized tissues as bone, horn, mollusc shells, tendon, cartilage, tooth enamel).

Individual evolution model

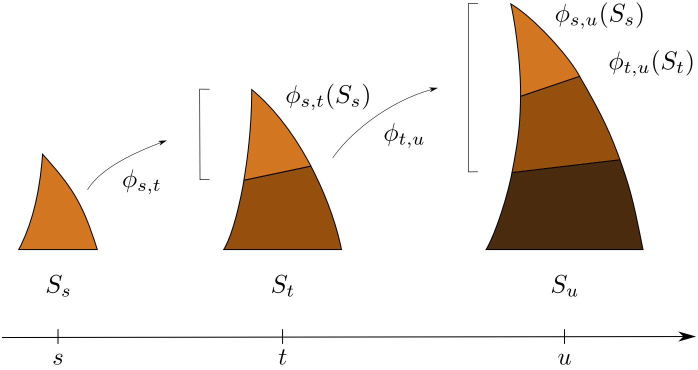

Creation processes call for inner partial mappings.

Def: a **growth scenario** is a curve of shapes, equipped with a flow of diffeomorphisms that

- define partial relations of homology between the ages of the shapes,
- allow the creation of new coordinates.

Population model

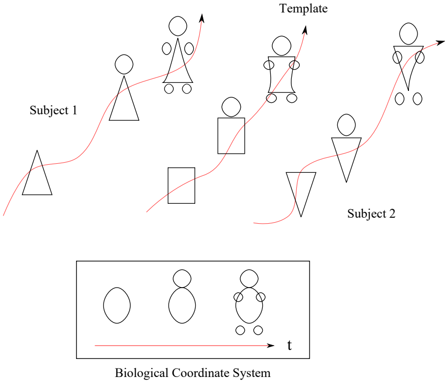

Shape spaces can be generalized for these growth scenarios. The metric results from the action of a group of spatio-temporal deformations.

New structuring hypothesis: a shape space of growth scenarios models a population of shape curves that share a common creation process.
This creation process is encoded by a biological coordinate system.

Time-dependent infinitesimal action

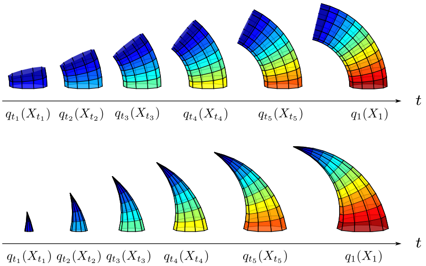

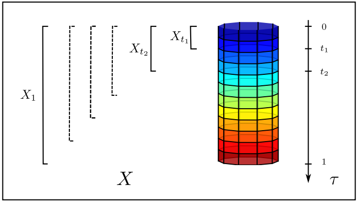

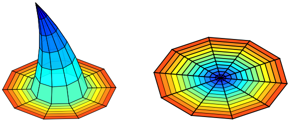

The biological coordinate system is the set of all the coordinates required to parametrize an individual growth scenario. These coordinates have a birth tag that allows to anticipate their emergence in the ambient space and to explicit the gradual embedding of the ages of the shape through the flow.

The action of a vector field is filtered by the birth tag

$$\forall t \in [0,1], \forall x \in X, \dot{q}_t(x) = \underbrace{\mathbb{1}_{\tau(x)\leq t}}_{\text{filter}} \underbrace{\boxed{v_t(q_t(x))\,.}}_{\text{standard infinitesimal action}}$$

Reconstitution of a scenario

We consider a population of scenarios, all aligned on the time interval $[0, 1]$. This population admits a common biological coordinate system (X, τ).

- The final shape S^{tar} of an individual's scenario is given.
- The initial position $q_0 : X \to \mathbb{R}^d$ is known.

Aim: We want to retrieve the complete scenario of this individual.

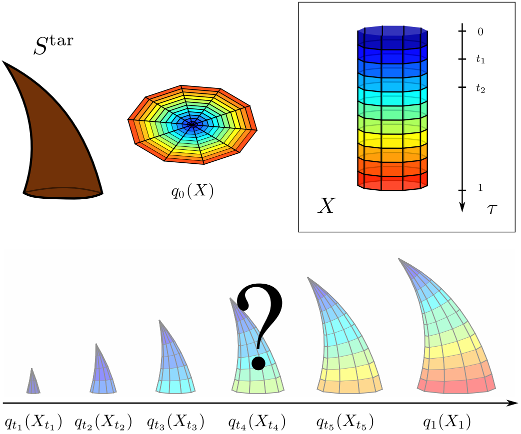

LDDMM: Gradient descent on the vector field

Inexact matching problem

Our aim is to find the *simplest* vector field $v^{opt} \in L^2_V$ such that $q_1(X)$ approximates the target shape S^{tar} *as well as possible*.

General minimization problem: $E : B \times L^2_V \to \mathbb{R}$

$$E(q_0, v) = \frac{1}{2} \int_0^1 |v_t|^2_V \, dt + \mathcal{A}(q_1) \quad \text{where } \dot{q}_t = \xi_{(q_t, t)}(v_t)\,.$$

Any minimizer must satisfy

$$v_t^{opt} = K^V \mathcal{J}(q_t, p_t, t)$$

where

$$\begin{array}{rcl} \mathcal{J} : B \times B^* \times [0,1] & \longrightarrow & V^* \\ (q, p, t) & \longmapsto & \xi^*_{(q,t)} \cdot p \end{array}$$

and $p_1 = -d\mathcal{A}(q_1) \in B^*$, $\dot{p}_t = -\partial_q \xi_{(q_t,t)}(v_t)^* \cdot p_t$.

Construction of a diffeomorphism with a RKHS

Example of deformation when the space of vector fields V is a Reproducing Kernel Hilbert Space with a Gaussian kernel. The vector field below is generated by 3 control points $(\delta_{x_i}^{p_i})_{i=1,2,3}$, pairs of positions and directions.

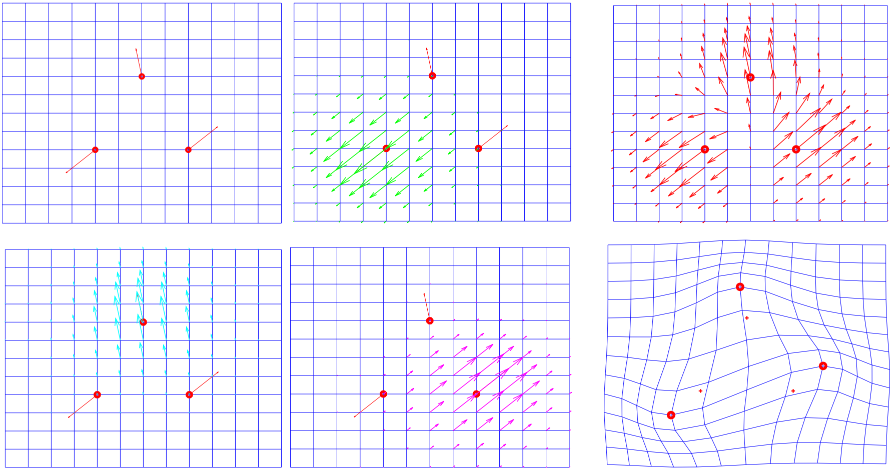

$\Rightarrow$ Large Deformation Diffeomorphic Metric Mapping (LDDMM) methods

Application

Superimposed trajectories of the solution and the target:

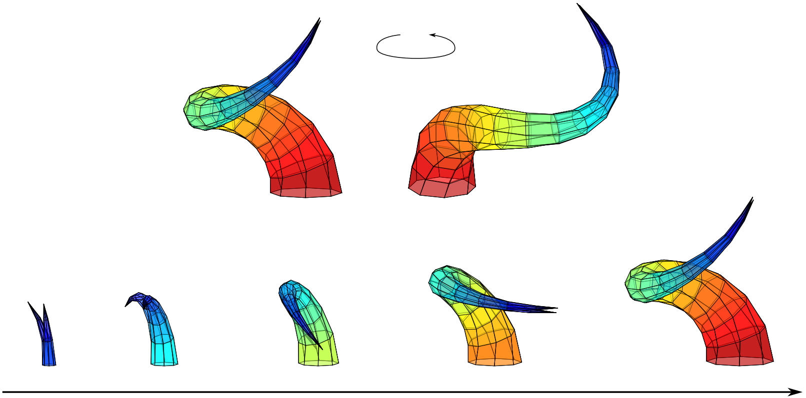

The continuous trajectory is completely determined by the initial position q_0 and the **initial momenta** p_0 (right figure).

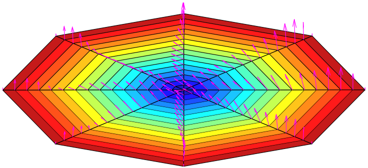

The end

Merci pour votre attention !

A penny for your thoughts:
What generic term for *currents*, *varifolds*, *oriented varifolds*, and *normal cycles* ?

Momentum and Momentum Map with the growth dynamic

With the growth dynamic, the momentum map builds the sum of the control points $\delta_{q(x)}^{p(x)}$ indexed by the active coordinates. The time variable t specifies the actual support $X_t \subset X$.

$$\mathcal{J}(q_t, p_t, t) = \sum_{x \in X_t} \delta_{q_t(x)}^{p_t(x)} ,$$

$$\begin{aligned} v_t^{opt} &= K^V \mathcal{J}(q_t, p_t, t) \\ &= \sum_{x \in X_t} k_V(q_t(x), \cdot) p_t(x) . \end{aligned}$$

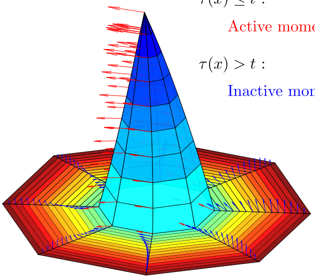

Examples:

$$v_t^{opt} = \sum_{x \in X_t} e^{-\frac{|q_t(x) - \cdot|^2}{2\sigma^2}} p_t(x) \qquad \text{or} \qquad v_t^{opt} = \sum_{x \in X_t} p_t(x) .$$

Variants of the minimization problem

For a large class of solutions $(q,p) \in \mathcal{C}([0,1], B \times B^*)$, $t \mapsto |v_t^{opt}|_V$ is **strictly increasing**. However, when the deformation are generated by global rotations and translations, we would like this norm to be rather constant.

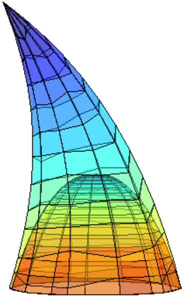

Flop.png

- **Adapted norm:**

$$E(q_0, v) = \frac{1}{2}\int_0^1 \alpha_t \, |v_t|_V^2 \; dt + \mathcal{A}(q_1)\,.$$

The minimizers of this energy satisfy

$$v_t^{opt} = \frac{1}{\alpha_t} K^V \mathcal{J}(q_t, p_t, t).$$

- **Constrained norm:** consider the classic energy

$$E(q_0, v) = \frac{1}{2}\int_0^1 |v_t|_V^2 \, dt + \mathcal{A}(q_1)\,,$$

and minimize it under the constraint that for any $t \in [0,1]$,

$$|v_t|_V^2 = c_t$$

where $c : [0,1] \to \mathbb{R}^+$ is known. (augmented Lagrangian method)

Non constant growth

Comparison of the norms of the vector fields between the target (red) and the solution (blue):

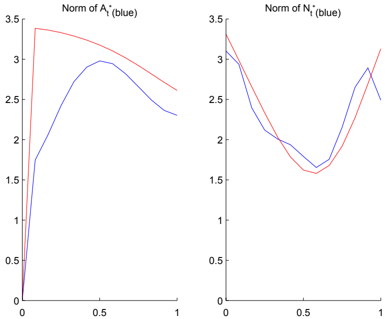

Adapted norm

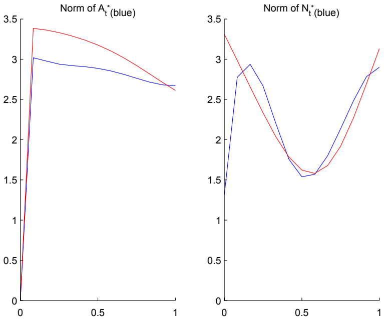

Constrained norm

Hamiltonian framework

For any minimizer $v^{opt} \in L^2_V$, the trajectory $(q, p) \in \mathcal{C}([0,1], B \times B^*)$ is solution of the system

$$\begin{cases} \dot{q}_t &= \frac{\partial H_r}{\partial p}(q_t, p_t, t) \\ \dot{p}_t &= -\frac{\partial H_r}{\partial q}(q_t, p_t, t) \end{cases}$$

where

$$H_r(q_t, p_t, t) = \frac{1}{2}|K^V \mathcal{J}(q_t, p_t, t)|^2_V \, .$$

The novelty here is that the Hamiltonian function depends on the time. Yet, it can be controlled by the initial condition (q_0, p_0).

It leads to a new minimization problem:

$$\hat{E}(q_0, p_0) = E(q_0, v) \quad \text{where } v_t = K^V \mathcal{J}(q_t, p_t, t) \, ,$$

and to a new algorithm (so-called *shooting method* on the initial momentum).